Acta Cryst. (1997). B53, 337–345

$Cu_{12}Sb_4S_{13}$: A Temperature-Dependent Structure Investigation

A. PFITZNER,[a]* M. EVAIN[b] AND V. PETRICEK[c]

[a]*Anorganische Chemie, Universität Siegen, D-57068 Siegen, Germany,* [b]*Laboratoire de Chimie des Solides IMN, UMR CNRS No.110, Université de Nantes, 2 rue de la Houssinière, 44072 Nantes CEDEX 03, France, and* [c]*Institute of Physics, Academy of Sciences of the Czech Republic, Na Slovance 2, 180 40 Praha 8, Czech Republic. E-mail: pfitzner@chemie.uni-siegen.d400.de*

(*Received 20 September 1996; accepted 11 November 1996*)

Abstract

Synthetic tetrahedrite, $Cu_{12}Sb_4S_{13}$, obtained by reaction of the elements, has been investigated at various temperatures in the 295–573 K range. It crystallizes in the cubic system with a = 10.3293 (6) Å, V = 1102.1 (2) Å^3, space group $I\bar{4}3m$ and Z = 2 at room temperature. The structure refinement converged to a residue of R = 0.0165 (at room temperature, wR = 0.0200) for 389 independent reflections and 34 refined parameters. A Gram–Charlier non-harmonic development of the atomic displacement factor for both independent Cu atoms was used. The results show a disorder for the three-coordinated Cu atom, within and perpendicular to the plane of the three surrounding S atoms. However, although the non-harmonic probability density deformation increases with raising the temperature within this plane, it barely changes in the perpendicular direction. This suggests two different types of disorder: static in-plane and dynamic out-of-plane, therefore underlining a possible diffusion pathway for copper ions. To check the significance of the observed effects, the errors for the one-particle potentials and the probability density function maps were calculated by means of a Monte-Carlo method.

1. Introduction

In nature tetrahedrite is a common sulfosalt with the nominal composition $M_{12}X_4S_{13}$, with M mainly Cu, but also, for instance, Zn, Fe, Hg, Ag and Pb, and with X = Sb and/or As. Recently, $Cu_{8.8}Te_4S_{13}$, a compound related to the tetrahedrite structure type, but containing neither Sb nor As, has been described (Kanatzidis & Sutorik, 1995). The tetrahedrite structure, which can be derived from the zinc blende structure, was first described by Pauling & Neuman (1934) and later refined by Wuensch (1964) from natural sample data. The natural samples have compositions that can vary in a wide range (*e.g.* Springer, 1969; Charnock, Garner, Pattrick & Vaughan, 1989) and even synthetic ternary tetrahedrite shows a certain composition range, from $Cu_{12}Sb_4S_{13}$ up to $Cu_{\sim 14}Sb_4S_{13}$, which strongly depends upon temperature (Bryndzia & Davis, 1989; Tatsuka & Morimoto, 1973; Skinner, Luce & Makovicky, 1972). At room temperature, for instance, a mixture of the tetrahedrite copper-poor and copper-rich immiscible phases is very often observed and above *ca* 373 K these two phases are reported to form a homogeneous solid solution (Tatsuka & Morimoto, 1973; Skinner, Luce & Makovicky, 1972). This 'exsolution process' might be one of the reasons why, up to now, no single crystal structure determination has been performed on stoichiometric $Cu_{12}Sb_4S_{13}$. To our knowledge the only report on the structure of a synthetic tetrahedrite has been given by Makovicky & Skinner (1979) who examined an intergrowth of the copper-poor and copper-rich compositions. Since the Cu atoms could not be easily localized in their structure determination, it was concluded that both phases, with compositions $Cu_{\sim 12.4}Sb_4S_{13}$ and $Cu_{\sim 13.8}Sb_4S_{13}$, show a high copper-ion mobility even at room temperature, which is in good agreement with the copper insertion experiments described by Tatsuka & Morimoto (1973).

In $Cu_{12}Sb_4S_{13}$ the two crystallographically independent Cu atoms have quite different sulfur coordinations. Indeed, one Cu atom occupies a tetrahedral void of S atoms and the second Cu atom is located in a sulfur triangle, exhibiting large anisotropic displacement parameters (ADP's). To ascertain the crystal structure of $Cu_{12}Sb_4S_{13}$ and to decide whether the unusually high ADP's of the three coordinated Cu atoms are due to dynamic effects or to a more or less static disorder, the temperature dependence of the crystal structure of $Cu_{12}Sb_4S_{13}$ was investigated. Refinements taking non-harmonic displacement parameters into account were carried out since, according to Bachmann & Schulz (1984), they should reveal the true nature of the large displacement parameters through an analysis of the temperature dependence of the one-particle pseudo-potential (OPP).

2. Experimental

2.1. *Synthesis*

Single crystals of $Cu_{12}Sb_4S_{13}$ were obtained from heating a stoichiometric mixture of the corresponding elements (Cu:Sb:S = 12:4:13), in sealed evacuated silica

ampoules at 873 K, and subsequent annealing at 673 K for several weeks. To improve the homogeneity of the samples two grinding procedures were carried out in between the annealing periods, but a small amount of the copper-rich phase was usually detectable by X-ray powder diffraction in the final product. No further phases, such as Cu_3SbS_3 (Pfitzner, 1994, and references therein; Makovicky & Balic-Zunic, 1995), known as skinnerite (Karup-Møller & Makovicky, 1974) and with a composition close to $Cu_{12}Sb_4S_{13}$, were detected.

2.2. *Data collection*

A good quality single crystal was selected and glued to the tip of a quartz capillary using a Torr Seal vacuum sealing kit. Diffraction intensities were collected at 295, 353, 423, 493 and 573 K on a Siemens P4 diffractometer equipped with an AET hot nitrogen gas-blowing device. The sample temperature was thus controlled within ±1 K. To avoid severe absorption effects that could lead to unreliable refinements, a graphite-monochromatized Ag radiation was used (λ = 0.56087 Å). The intensity decay observed during the high-temperature measurements was less than 5% for each temperature; however, at 643 K the crystal decomposed within several hours. To minimize expansion effects of the goniometer head, the data collections were performed in an azimuthal mode with a 5° ψ angle. For data collection details, see Table 1.*

2.3. *Data processing*

During the data reduction procedures of the different data sets only one reflection was excluded due to an asymmetric background. The measured intensities were obtained by fitting of the reflection profiles. They were corrected for scale variations by means of three standard reflections, and for Lorentz and polarization effects. A semi-empirical absorption correction based upon ψ-scans was then applied. Symmetry-equivalent reflections were merged according to the point group $\bar{4}3m$ with a typical R_{int} = 0.040 (295 K dataset). The whole data reduction procedure was performed with the *XSCANS*™ and *SHELXTL*™ software packages. For the refinements, Fourier syntheses and contour plots the *JANA*96 program package (Petricek, 1996) was used. A Gram–Charlier expansion of the non-harmonic ADP's up to the fourth order (Johnson & Levy, 1974) was used for the two independent Cu atoms. Scattering factors and correction terms for anomalous dispersion were taken from Cromer & Waber (1974) and Cromer (1974), respectively. During the full-matrix least-squares refinement of the atomic parameters, the scale factor and an isotropic extinction coefficient [type I, Lorentzian distribution (Becker & Coppens, 1974)], the function $wR = [\Sigma w(|F_o| - |F_c|)^2/\Sigma w|F_o|^2]^{1/2}$ was minimized. All reflections with $\sin\theta/\lambda \leq 0.75$ were included and a weighting factor w based on $\sigma(F_o)$ with an additional instability coefficient was chosen (see Table 1 for details).

3. Results

In a first stage the composition of the crystal under investigation had to be determined with accuracy. A refinement of all occupation factors except that of antimony immediately showed that all sites are completely occupied within a 1σ level. Indeed, taking the harmonic ADP's into account the R value converged to 0.0194 for full occupation of the sites and to 0.0191 with the refinement of the occupation factors, *i.e.* after the introduction of four additional parameters. The refined composition was then $Cu_{11.98}Sb_4S_{12.99}$, with e.s.d.'s of 0.04 and 0.05 for copper and sulfur, respectively. Therefore, in the subsequent refinements a full occupation of all sites was assumed and occupancies were not refined. At this stage, the Flack parameter (Flack, 1983; Bernardinelli & Flack, 1985), refined to x = 0.07 (6) using *SHELXL*93 (Sheldrick, 1993), proved the use of the correct polarity. Then, to obtain more information concerning the large ADP's of Cu(2) perpendicular to the plane of the three coordinating S atoms, several models were compared. For only one refined Cu(2) position and harmonic ADP's a residue of R = 0.0194 was obtained. This model was slightly improved (R = 0.0191) by splitting the Cu(2) position into two sites with isotropic displacement parameters (IDP's) in the centre and at the top of the original ellipsoid, and then ameliorated (R = 0.0178) by refining only the central position anisotropically. Including non-harmonic ADP's up to the fourth order for just one Cu(2) position gave similar results (R = 0.0172). This last model, although using more variables (27 *versus* 22 for the best split model), was preferred since it drastically reduced the correlation coefficients (0.866 *versus* 0.994 for the split model) and presented more flexibility for the refinements of the high-temperature data sets (*vide infra*). The same development of the temperature factor (fourth order) was introduced for the second Cu atom, which led to the final residue of R = 0.0165 (wR= 0.0170). Since the non-harmonic probability density function (p.d.f.) sections (*vide infra*) show no significant negative regions, the model can be regarded as valid (Bachmann & Schulz, 1984). The refined atomic site parameters are given in Table 2.

The same procedure was applied to the high-temperature datasets (see Table 1 for the refinement results and Table 2 for the atomic positions at 573 K). For comparison the ADP's (up to the second order for copper) at 295 and 573 K are listed in Table 3. The third- and fourth-order ADP's for Cu atoms are summarized in Table 4. Table 5 contains selected interatomic distances (based upon the mean positions) at 295 and 573 K.

* A list of structure factors has been deposited with the IUCr (Reference: SE0205). Copies may be obtained through The Managing Editor, International Union of Crystallography, 5 Abbey Square, Chester CH1 2HU, England.

Table 1. *Experimental details*

	295 K	353 K	423 K	493 K	573 K
Crystal data					
Chemical formula	$Cu_{12}Sb_{13}S_4$	$Cu_{12}Sb_{13}S_4$	$Cu_{12}Sb_{13}S_4$	$Cu_{12}Sb_{13}S_4$	$Cu_{12}Sb_{13}S_4$
Chemical formula weight	1666.33	1666.33	1666.33	1666.33	1666.33
Cell setting	Cubic	Cubic	Cubic	Cubic	Cubic
Space group	$I\bar{4}3m$	$I\bar{4}3m$	$I\bar{4}3m$	$I\bar{4}3m$	$I\bar{4}3m$
a (Å)	10.3293 (6)	10.3363 (5)	10.3424 (7)	10.3523 (6)	10.3678 (7)
V (Å^3)	1102.1 (2)	1104.3 (2)	1106.3 (2)	1109.5 (2)	1114.5 (2)
Z	2	2	2	2	2
D_x (Mg m^{-3})	5.020	5.010	5.001	4.986	4.964
Radiation type	Ag K–$L_{2,3}$	Ag K–$L_{2,3}$	Ag K–$L_{2,3}$	Ag K–$L_{2,3}$	Ag K–$L_{2,3}$
Wavelength (Å)	0.56087	0.56087	0.56087	0.56087	0.56087
No. of reflections for cell parameters	26	22	22	22	22
θ range (°)	5.4–15.4	5.4–15.4	5.4–15.4	5.4–15.4	5.4–15.4
μ (mm^{-1})	8.973	8.955	8.939	8.913	8.873
Temperature (K)	295	353	423	493	573
Crystal form	Irregular	Irregular	Irregular	Irregular	Irregular
Crystal size (mm)	0.25 × 0.20 × 0.18	0.25 × 0.20 × 0.18	0.25 × 0.20 × 0.18	0.25 × 0.20 × 0.18	0.25 × 0.20 × 0.18
Crystal colour	Metallic black	Metallic black	Metallic black	Metallic black	Metallic black
Data collection					
Diffractometer	Siemens P4	Siemens P4	Siemens P4	Siemens P4	Siemens P4
Monochromator	Oriented graphite	Oriented graphite	Oriented graphite	Oriented graphite	Oriented graphite
Data collection method	Profile-fitted ω scans	Profile-fitted ω scans	Profile-fitted ω scans	Profile-fitted ω scans	Profile-fitted ω scans
Absorption correction	ψ-scan (Sheldrick, 1996)	ψ-scan (Sheldrick, 1996)	ψ-scan (Sheldrick, 1996)	ψ-scan (Sheldrick, 1996)	ψ-scan (Sheldrick, 1996)
T_{min}	0.61	0.61	0.61	0.61	0.61
T_{max}	0.82	0.82	0.82	0.82	0.82
No. of measured reflections	3000	3532	2881	2880	2905
No. of independent reflections	538	643	538	542	542
No. of observed reflections	389	393	391	387	383
Criterion for observed reflections	$I > 1\sigma(I)$	$I > 1\sigma(I)$	$I > 1\sigma(I)$	$I > 1\sigma(I)$	$I > 1\sigma(I)$
R_{int}	0.041	0.043	0.042	0.058	0.058
θ_{max} (°)	27.96	29.91	27.93	27.96	27.93
sin $(\theta/\lambda)_{max}$	0.836	0.889	0.835	0.836	0.835
Range of h, k, l	$-15 \rightarrow h \rightarrow 15$ $-17 \rightarrow k \rightarrow 17$ $-17 \rightarrow l \rightarrow 17$	$-18 \rightarrow h \rightarrow 19$ $-17 \rightarrow k \rightarrow 17$ $-18 \rightarrow l \rightarrow 18$	$-15 \rightarrow h \rightarrow 15$ $-16 \rightarrow k \rightarrow 16$ $-17 \rightarrow l \rightarrow 17$	$-14 \rightarrow h \rightarrow 15$ $-16 \rightarrow k \rightarrow 16$ $-17 \rightarrow l \rightarrow 17$	$-15 \rightarrow h \rightarrow 15$ $-16 \rightarrow k \rightarrow 16$ $-17 \rightarrow l \rightarrow 17$
No. of standard reflections	3	3	3	3	3
Frequency of standard reflections	Every 100 reflections	Every 100 reflections	Every 100 reflections	Every 100 reflections	Every 100 reflections
Intensity decay (%)	<1	<1	<1	3	4
Refinement					
Refinement on	F	F	F	F	F
$R(F)$	0.0165	0.0180	0.0188	0.0253	0.0248
$wR(F)$	0.0200	0.0210	0.0222	0.0312	0.0292
S	1.11	1.21	1.24	1.65	1.47
No. of reflections used in refinement	389	393	391	387	383
No. of parameters used	34	34	34	34	34
Weighting scheme	$w = 1/[\sigma^2(\lvert F_o\rvert^2) + (0.01\lvert F_o\rvert^2)^2]$	$w = 1/[\sigma^2(\lvert F_o\rvert^2) + (0.01\lvert F_o\rvert^2)^2]$	$w = 1/[\sigma^2(\lvert F_o\rvert^2) + (0.01\lvert F_o\rvert^2)^2]$	$w = 1/[\sigma^2(\lvert F_o\rvert^2) + (0.01\lvert F_o\rvert^2)^2]$	$w = 1/[\sigma^2(\lvert F_o\rvert^2) + (0.01\lvert F_o\rvert^2)^2]$
$(\Delta/\sigma)_{max}$	<0.0001	<0.0001	<0.0001	<0.0001	<0.0001
$\Delta\rho_{max}$ (e Å^{-3})	0.72	0.48	0.39	0.76	0.50
$\Delta\rho_{min}$ (e Å^{-3})	−0.85	−0.55	−0.45	−0.76	−0.83
Extinction method	Secondary isotropic	Secondary isotropic	Secondary isotropic	Secondary isotropic	Secondary isotropic
Extinction coefficient	0.27 (1)	0.34 (1)	0.34 (1)	0.31 (2)	0.23 (1)
Source of atomic scattering factors	*International Tables for X-ray Crystallography* (1974, Vol. IV)	*International Tables for X-ray Crystallography* (1974, Vol. IV)	*International Tables for X-ray Crystallography* (1974, Vol. IV)	*International Tables for X-ray Crystallography* (1974, Vol. IV)	*International Tables for X-ray Crystallography* (1974, Vol. IV)

$R(F) = \sum\{\lvert\lvert F_o\rvert - \lvert F_c\rvert\rvert\}/\sum\lvert F_o\rvert$; $wR(F) = \{\sum[w(\lvert F_o\rvert - \lvert F_c\rvert)^2]/\sum(w\lvert F_o\rvert^2)\}^{1/2}$; $S = \{\sum[w(\lvert F_o\rvert - \lvert F_c\rvert)^2]/N - P\}^{1/2}$.

Since the number of parameters *versus* the number of reflections ratio was sufficient, all symmetrically independent non-harmonic tensor elements were refined according to their site-symmetry restrictions (Kuhs, 1984), despite the fact that many of them were negligible within a 3σ cut-off.

Table 2. *Fractional atomic coordinates and equivalent isotropic displacement parameters (Å²)*

$U_{eq} = (1/3)\Sigma_i\Sigma_j U^{ij} a_i^* a_j^* \mathbf{a}_i.\mathbf{a}_j$.

	x	y	z	U_{eq}
295 K				
Cu(1)	1/2	0.0	1/4	0.0245 (5)
Cu(2)	0.0	0.0	0.2178 (2)	0.0615 (6)
Sb	0.26870 (3)	0.26870 (3)	0.26870 (3)	0.01728 (8)
S(1)	−0.11601 (7)	−0.11601 (7)	0.36309 (9)	0.0174 (2)
S(2)	0.0	0.0	0.0	0.0251 (4)
573 K				
Cu(1)	1/2	0.0	1/4	0.048 (1)
Cu(2)	0.0	0.0	0.2168 (3)	0.090 (1)
Sb	0.26776 (4)	0.26776 (4)	0.26776 (4)	0.0305 (2)
S(1)	−0.1155 (1)	−0.1155 (1)	0.3624 (1)	0.0303 (3)
S(2)	0.0	0.0	0.0	0.0368 (6)

Table 3. *Anisotropic thermal displacement parameters U^{ij} (Å²) for $Cu_{12}Sb_4S_{13}$ at 295 and 573 K*

The anisotropic thermal displacement factor exponent takes the form: $(-2\pi^2 \sum_i \sum_j U^{ij} |a_i^*||a_j^*| h_i h_j)$.

	$U^{11} = U^{22}$	U^{33}	U^{12}	U^{13}	U^{23}
295 K					
Cu(1)	0.0222 (5)	0.029 (1)	0.0	0.0	0.0
Cu(2)	0.079 (1)	0.026 (1)	−0.049 (2)	0.0	0.0
Sb	0.0173 (1)	U^{11}	−0.0010 (1)	U^{12}	U^{12}
S(1)	0.0182 (2)	0.0160 (4)	0.0010 (3)	−0.0020 (2)	U^{13}
S(2)	0.0251 (6)	U^{11}	0.0	0.0	0.0
573 K					
Cu(1)	0.0424 (9)	0.060 (3)	0.0	0.0	0.0
Cu(2)	0.113 (2)	0.042 (2)	−0.054 (3)	0.0	0.0
Sb	0.0305 (2)	U^{11}	−0.0023 (3)	U^{12}	U^{12}
S(1)	0.0322 (5)	0.0264 (7)	0.0003 (6)	−0.0029 (4)	U^{13}
S(2)	0.037 (1)	U^{11}	0.0	0.0	0.0

Difference-Fourier maps at 295 K around the Cu(2) site before and after the introduction of non-harmonic ADP's are shown in Fig. 1. It is worth noticing that the positive peak in the x direction [*i.e.* in the S(2) direction] could not be explained, neither by the classical harmonic model nor by our split model (*vide supra*). The non-harmonic deformation density (p.d.f.$_{def}$) for Cu(2), already visible at room temperature, becomes more and more pronounced with increasing temperature. The same results are observed for Cu(1), but since the coordination tetrahedron is more regular (sphere-like), the effects are not as pronounced.

4. Discussion

Two different fragments of the crystal structure of $Cu_{12}Sb_4S_{13}$ are shown in Fig. 2. As already discussed by Pauling & Neuman (1934) and Wuensch (1964), the structure can be derived from the sphalerite-type, but the coordination for the metal atoms is no longer a tetrahedron in all cases. Instead, a tetrahedral $[Cu(1)S(1)_{4/4}]$, a trigonal pyramidal $[SbS(1)_{3/4}]$ and a trigonal planar $[Cu(2)S(1)_{2/4}S(2)_{1/6}]$ group are the basic building units of the tetrahedrite structure. The coordination polyhedra for the S atoms are on the one hand a tetrahedron $[S(1)Sb_{1/3}Cu(1)_{2/4}Cu(2)_{1/3}]$ (see Fig. 2*a*) and on the other hand an octahedron $[S(2)Cu(2)_{6/3}]$ (see Fig. 2*b*).

Three-dimensional (3D) isosurfaces of the non-harmonic p.d.f. for Cu(1) and Cu(2) are presented in Fig. 3. The non-harmonic p.d.f. for Cu(1) shows

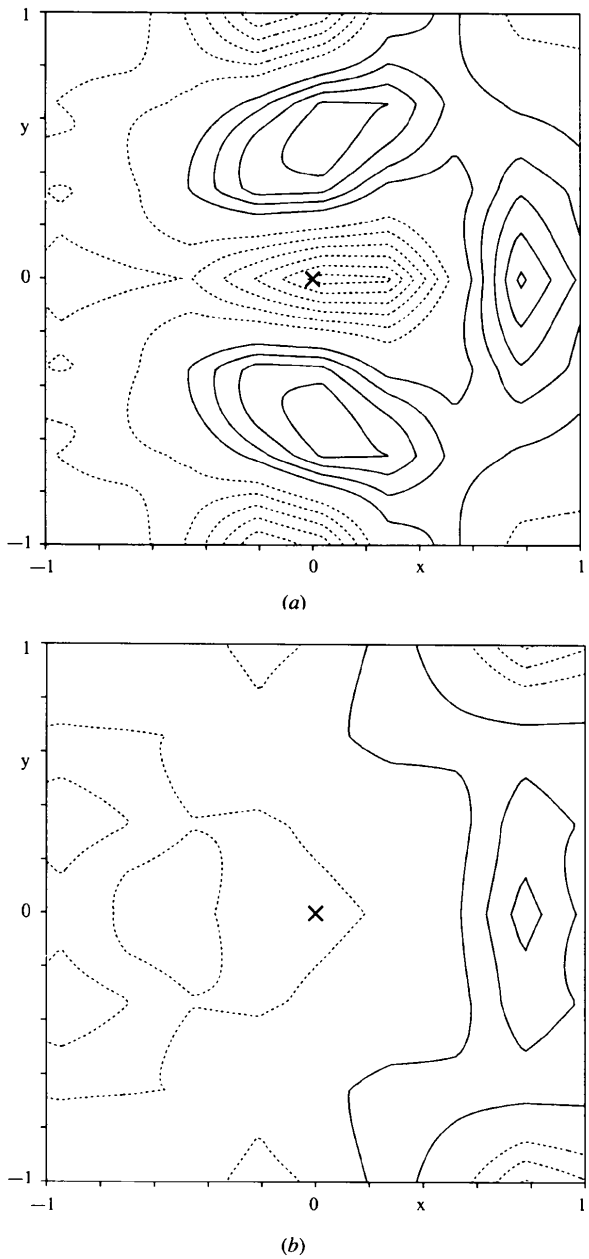

Fig. 1. Difference-Fourier sections at 295 K through the Cu(2) site, in the plane defined by the neighbouring S(2) and Sb atoms. (*a*) After harmonic anisotropic refinement and (*b*) after introduction of non-harmonic ADP's up to the fourth order. The Cu(2) atomic position is indicated by a cross; contour levels 0.1 e Å^{-3}.

Table 4. *Non-harmonic displacement parameters for the Cu atoms at various temperatures*

Third-order elements C_{pqr} are multiplied by 10^5; fourth-order tensor elements D_{pqrs} are multiplied by 10^6.

	295 K		353 K		423 K		493 K		573 K	
	Cu(1)	Cu(2)	Cu(1)	Cu(2)	Cu(1)	Cu(2)	Cu(1)	Cu(2)	Cu(1)	Cu(2)
C_{113}	0.01 (1)	−0.07 (2)	0.02 (1)	−0.13 (3)	−0.02 (1)	−0.18 (3)	0.02 (2)	−0.24 (5)	0.10 (3)	−0.21 (5)
C_{123}	−0.02 (1)	0.01 (3)	−0.04 (1)	0.03 (3)	−0.06 (2)	0.03 (3)	−0.11 (3)	0.04 (5)	−0.17 (3)	−0.08 (6)
C_{223}	$-C_{113}$	C_{113}	$-C_{113}$	C_{113}	$-C_{113}$	C_{113}	$-C_{113}$	C_{113}	$-C_{113}$	C_{113}
C_{333}		0.02 (3)		0.19 (4)		0.13 (4)		0.18 (7)		0.19 (7)
D_{1111}	0.02 (1)	−0.27 (3)	0.06 (1)	−0.35 (3)	0.05 (1)	−0.46 (4)	0.03 (2)	−0.49 (7)	0.03 (3)	−0.52 (8)
D_{1112}	0.004 (6)	0.22 (3)	−0.008 (7)	0.27 (3)	0.002 (8)	0.33 (3)	0.01 (1)	0.28 (6)	0.01 (1)	0.27 (7)
D_{1122}	0.020 (6)	−0.22 (3)	0.036 (7)	−0.23 (3)	0.023 (8)	−0.25 (4)	0.03 (1)	−0.18 (6)	0.04 (1)	−0.10 (7)
D_{1133}	0.019 (6)	0.00 (1)	0.004 (7)	−0.01 (1)	0.005 (8)	−0.04 (1)	−0.01 (1)	−0.03 (2)	0.05 (2)	−0.04 (3)
D_{1222}	$-D_{1112}$	D_{1112}	$-D_{1112}$	D_{1112}	$-D_{1112}$	D_{1112}	$-D_{1112}$	D_{1112}	$-D_{1112}$	D_{1112}
D_{1233}		0.00 (1)		0.02 (1)		0.02 (2)		0.05 (3)		0.06 (3)
D_{2222}	D_{1111}	D_{1111}	D_{1111}	D_{1111}	D_{1111}	D_{1111}	D_{1111}	D_{1111}	D_{1111}	D_{1111}
D_{2233}	D_{1133}	D_{1133}	D_{1133}	D_{1133}	D_{1133}	D_{1133}	D_{1133}	D_{1133}	D_{1133}	D_{1133}
D_{3333}	0.00 (3)	0.01 (3)	0.08 (3)	0.11 (4)	0.10 (4)	0.11 (4)	0.06 (6)	0.18 (7)	0.37 (10)	0.09 (7)

Table 5. *Selected interatomic distances (Å) and angles (°) for $Cu_{12}Sb_4S_{13}$ at 295 and 573 K, and, for comparison, for $Cu_{12.3}Sb_4S_{13}$ and $Cu_{10.4}Zn_{1.2}Fe_{0.3}S_{13}$, respectively*

		295 K (this work)	573 K (this work)	$Cu_{12.3}Sb_4S_{13}$ (Makovicky & Skinner, 1979)	$Cu_{10.4}Zn_{1.2}Fe_{0.3}S_{13}$ (Wuensch, 1964)
Cu(1)—S(1)	4×	2.3133 (8)	2.326 (1)	2.311 (4)	2.342 (4)
Cu(2)—S(1)	2×	2.264 (2)	2.269 (3)	2.246 (7)	2.272 (10)
Cu(2)—S(2)		2.249 (2)	2.248 (3)	2.250 (6)	2.234 (5)
Cu(2)—Cu(2)	4×	3.181 (2)	3.180 (3)	3.186 (8)	3.159 (8)
Cu(2)—Sb	2×	3.3818 (3)	3.4090 (4)	3.386	3.411
Sb—S(1)	3×	2.4342 (8)	2.438 (1)	2.452 (4)	2.446 (7)
S(1)—Cu(1)—S(1)	2×	106.51 (3)	106.37 (4)	105.45 (15)	106.50 (20)
	4×	110.97 (3)	111.04 (4)	111.52 (15)	110.97 (15)
S(1)—Cu(2)—S(1)		96.9 (1)	96.6 (1)	96.04 (25)	96.31 (30)
S(1)—Cu(2)—S(2)	2×	131.54 (5)	131.70 (7)	131.98 (10)	131.85 (15)
Sb—Cu(2)—Sb		175.26 (8)	174.6 (1)	175.2	174.1
S(1)—Sb—S(1)	3×	95.70 (3)	95.87 (4)	95.70 (10)	95.13 (25)

a typical temperature behaviour for a tetrahedrally coordinated atom (*e.g.* Oliveria, McMullan & Wuensch, 1988; Pfitzner & Lutz, 1993; Yude, Boysen & Schulz, 1990), *i.e.* a main deformation towards the tetrahedron faces (see Fig. 3*a*). This behaviour for Cu^+ has been discussed in terms of a second-order Jahn–Teller effect (*e.g.* Burdett & Eisenstein, 1992), *i.e.* a mixing of the copper 3*d*/4*s* orbitals. However, a thorough analysis of the density deformation indicates a slight enhancement in the direction of the interstitial copper positions found in the copper-rich tetrahedrite $Cu_{13}Sb_4S_{13}$ (Pfitzner, 1996). For Cu(2), located in a triangular plane of S atoms, a relatively large non-harmonic displacement perpendicularly to the sulfur plane is observed, in agreement with previous observations for similar atomic arrangements (*e.g.* Daoudi, Lamire, Levet & Noël, 1996; Gotsis, Barnes & Strange, 1992; Pfitzner, 1994, and references therein). However, a less important but strongly non-harmonic displacement within the sulfur triangle is also observed. This is certainly to be related to the irregularity of the sulfur triangle coordinating Cu(2), the *d*(S—S) distances being quite different, namely *d*[S(1)—S(1)] = 3.389 (1) and *d*[S(1)—S(2)] = 4.1154 (9) Å at 295 K. The Cu(2) p.d.f. section at 295 K presented in Fig. 4(*a*) shows that the main directions of the Cu(2) density deformation are the longer edges of the sulfur triangle, more precisely the directions of the interstitial Cu atoms found in the copper-rich tetrahedrites (*vide supra*). At higher temperature, the density deformation towards the three S—S edges, even the shorter one, is enhanced (see Figs. 4*b* and *c*).

Our last analysis seems to indicate an important evolution of the Cu(2) p.d.f. as a function of temperature. To characterize that evolution and conclude upon the nature of the disorder, one-particle potentials were calculated along two directions defined by Cu(2) and Sb, and Cu(2) and S(2), respectively. They are presented as a function of temperature in Figs. 5(*a*) and (*b*), respectively. The OPP perpendicular to the sulfur plane and along the Cu(2)—Sb direction (Fig. 5*a*) is very flat. The shapes of

the potential curves and especially of their derivatives (not shown) indicate a large delocalization towards the two Sb atoms, although not resolved in the temperature range of our study. A typical behaviour for a d^{10} element in a threefold sulfur coordination is illustrated by Ag^+ in $Ag_2MnP_2S_6$ (Van der Lee, Boucher, Evain & Brec, 1993). At low temperature the potential is non-harmonic and rather flat, indicating a certain delocalization of the d^{10} ion above and below the sulfur triangle. As the temperature increases, the d^{10} element tends to move to higher coordination sites, giving a resolved disorder characterized by a double well potential. However, this movement can be prevented by a repulsive interaction with another cation. Indeed, in $Ag_2MnP_2S_6$ the Ag^+ d^{10} element moves on one side of the sulfur triangle towards a tetrahedral site (the disorder is resolved and the potential presents a double minimum), but cannot be displaced on the other side because of the presence of a neighbouring Ag ion (the disorder is not resolved and

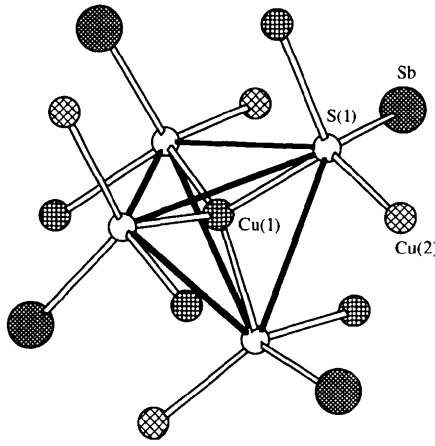

(*a*)

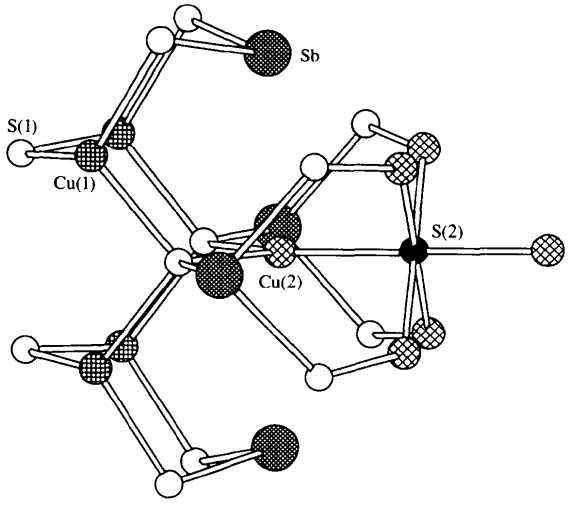

(*b*)

Fig. 2. Views of the crystal structure of $Cu_{12}Sb_4S_{13}$ showing (*a*) the tetrahedral coordination for Cu(1) and (*b*) the trigonal planar surrounding for Cu(2) and the octahedrally coordinated S(2).

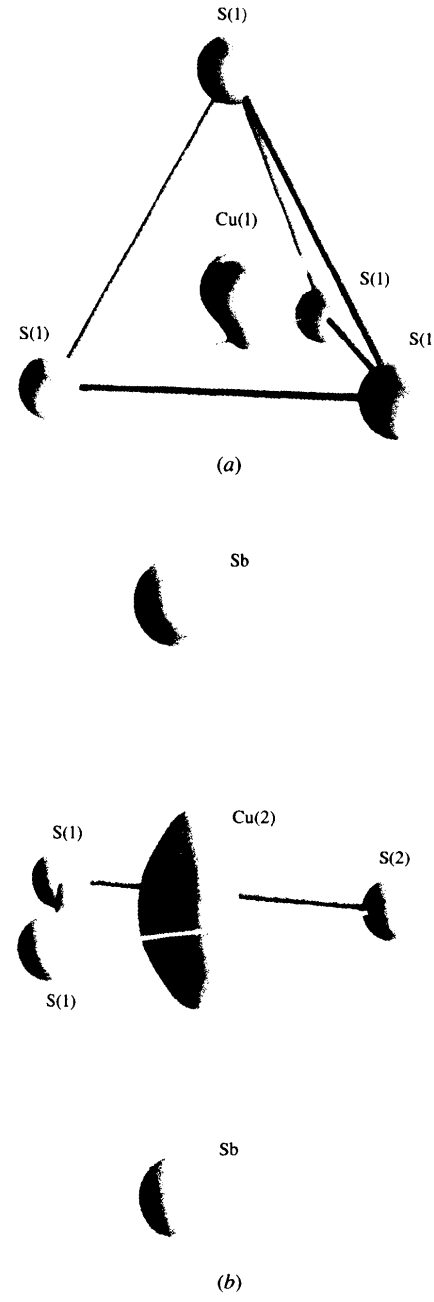

Fig. 3. 3D surface plots of the p.d.f. at 573 K of (*a*) Cu(1) and (*b*) Cu(2). The surrounding Sb atoms seem to influence the delocalization behaviour of Cu(2) perpendicularly to the plane defined by the three S atoms. Notice that the deformation of Cu(1) is less pronounced than that of Cu(2).

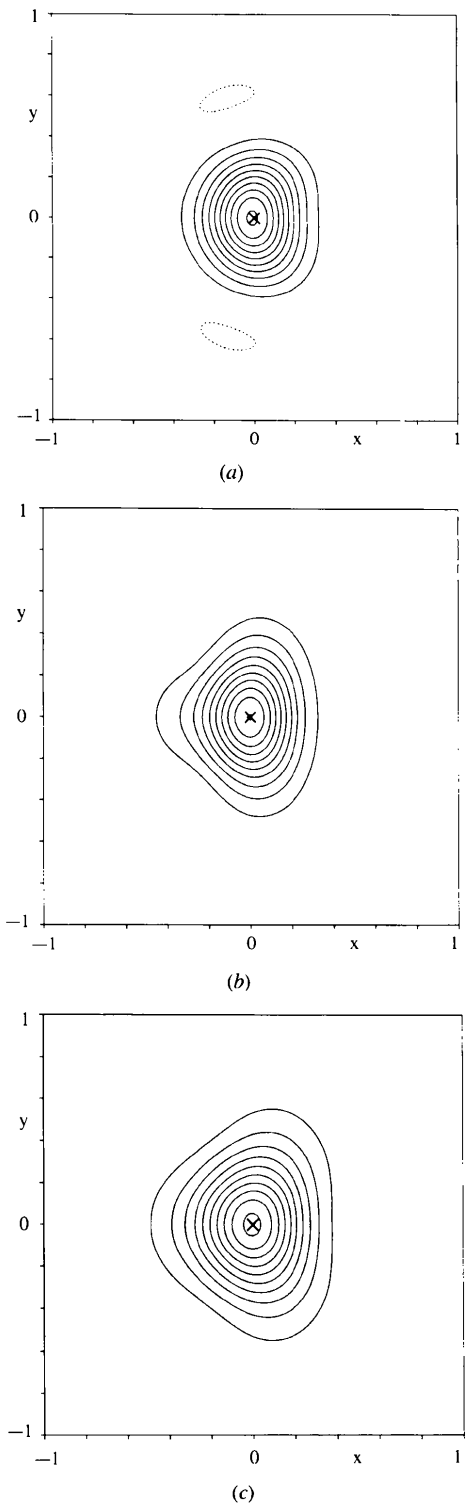

Fig. 4. The p.d.f. maps for Cu(2) in the plane at (*a*) 295, (*b*) 423 and (*c*) 573 K, showing the increasing probability density in the direction of the edges of the sulfur triangle. (*a*) Min/max density: −16/6088 Å^{-3}, step: −10/+600 Å^{-3}; (*b*) min/max density: −7/4816 Å^{-3}, step: +480 Å^{-3}; (*c*) min/max density: 0/3493 Å^{-3}, step: +340 Å^{-3}.

the potential remains flat). In $Cu_{12}Sb_4S_{13}$ the situation seems to follow that general trend. At 295 K Cu(2) is delocalized on both sides of the triangle (see Fig. 3*b*) and the potential is non-harmonic and flat. As the temperature increases it would move out of the triangle plane towards higher coordination sites, but is prevented from doing so by a repulsive interaction with antimony on both sides of the plane, therefore, the potential remains flat. That frustration could explain the important p.d.f.$_{def}$ within the sulfur plane at high temperature, a phenomenon not observed in $Ag_2MnP_2S_6$. The OPP along the Cu(2)—S(2) direction, within the sulfur plane (Fig. 5*b*), exhibits different features. At 295 K it is close to a harmonic one. Then, above 295 K, a transition seems to occur. Structures appear on both sides, being more pronounced towards S(2). These features, which are characteristic of an unresolved static disorder, have been demonstrated to be significant (see *Appendix*). They vanish at high temperature, a classical situation already described by Bachmann & Schulz (1984). The significant change above 295 K might be related to the formation of the solid solution range, already mentioned in the *Introduction* (Skinner, Luce & Makovicky, 1972; Tatsuka & Morimoto, 1973).

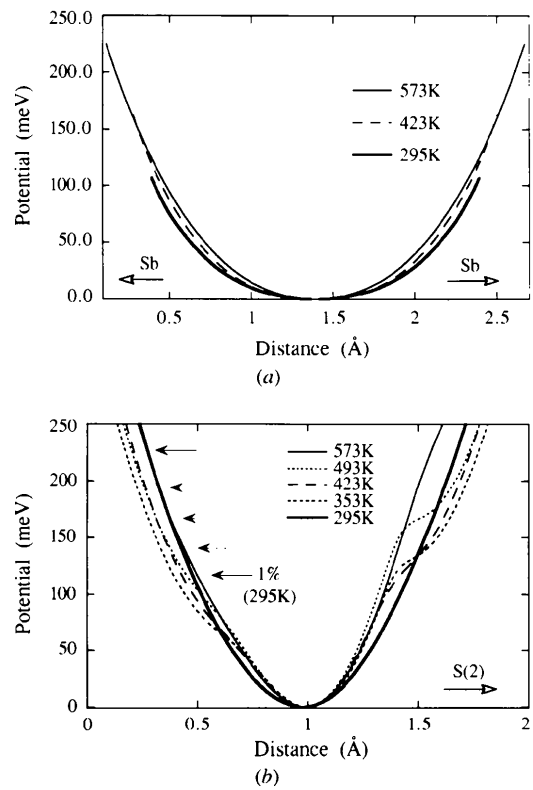

Fig. 5. Effective OPP derived from the non-harmonic p.d.f. for Cu(2). (*a*) Direction defined by Cu(2) and Sb; (*b*) direction defined by Cu(2) and S(2). The 1% cut-off according to the Boltzman statistics is indicated for each temperature.

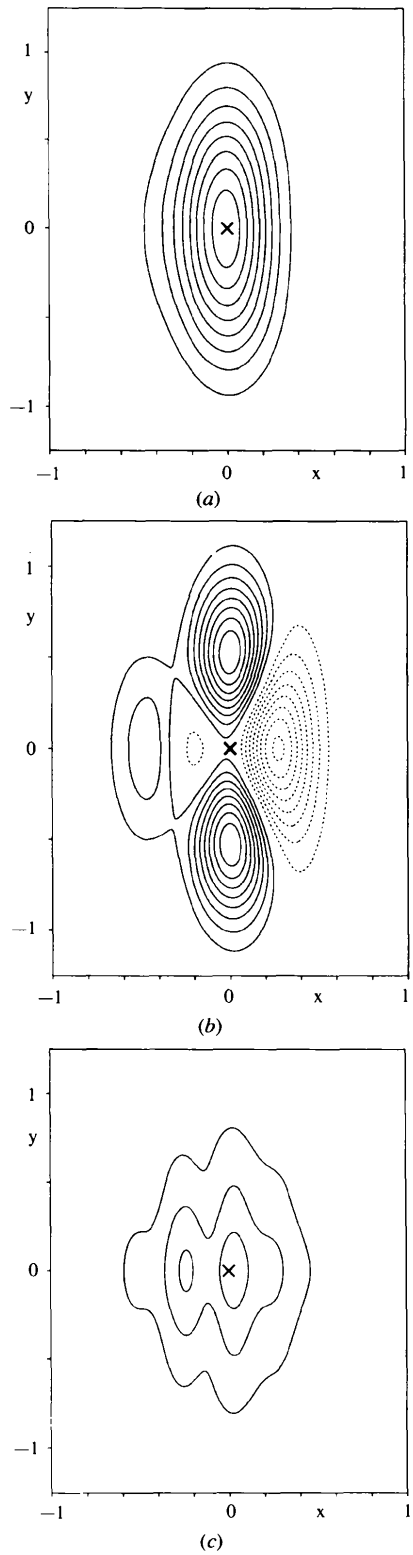

Fig. 6. (*a*) The p.d.f. map for Cu(2) at 573 K in the plane defined by S(2) and Sb, min/max density: −2/3493 Å^{-3}, step: +400 Å^{-3}; (*b*) p.d.f.$_{def}$ map, min/max density: −410/+442 Å^{-3}, step: ±40 Å^{-3}; (*c*) error map for the p.d.f. with an accuracy of 1%, step: ±40 Å^{-3}.

5. Conclusions

The crystal structure of stoichiometric tetrahedrite $Cu_{12}Sb_4S_{13}$ was determined for the first time. The refinement of the occupation factors is in good agreement with preliminary results from electrochemical lithium intercalation experiments and band structure calculations (Boucher, Evain, Deniard & Pfitzner, 1996), which suggest a deficit of two electrons per formula unit in the valence band. By means of temperature-dependent X-ray structure analyses taking non-harmonic tensors up to the fourth order for copper into account, no phase transitions for $Cu_{12}Sb_4S_{13}$ up to 573 K were detected. However, the in-plane effective OPP for the three-coordinated Cu atom shows a significant step-like change in the medium temperature range. The structure analyses up to 573 K give no hints for a high ionic mobility of copper over a wide range of the crystal structure, but from the shape of the Cu atom p.d.f. maps a preferred pathway for an ionic conduction can be derived, in relation to the position of the interstitial Cu atoms in the copper-rich tetrahedrites. This diffusion path should become clearer at higher temperatures, but unfortunately it was impossible to collect data above 573 K. Additional experiments, for instance, solid-state NMR measurements at high temperatures, are necessary to prove the high ionic conductivity in $Cu_{12}Sb_4S_{13}$. The analysis of the effective OPP for Cu(2) perpendicular to the plane of the coordinating S atoms can be discussed in terms of repulsive interactions between Cu(2) and Sb, leading to an increasing delocalization of copper in the plane defined by the S atoms.

AP is gratefully indebted to Professor Deiseroth for his continuous support of this work. The research of VP has been made possible by a grant from the French CNRS. VP also thanks the Grant Agency of the Czech Republic (grant no. 202/96/0085).

APPENDIX *A*

Since non-harmonic effects on the p.d.f. of copper are weak (compared with those observed for silver for instance), special care was taken for the determination of the corresponding e.s.d.'s. A method based on propagation of errors, excluding all covariances, can just give a rough estimation of the e.s.d.'s, even when correlations are smaller than 0.9. However, such an approximation is completely useless for j.p.d.f. maps, where correlations are usually strong. The generalization of the propagation law for the full variance–covariance matrix is very cumbersome. Therefore, the Monte-Carlo method, as first described by Kuhs (1992), is probably the only method which can solve this problem in a general way. With such a method it is possible to calculate error maps, taking into account not only the full variance–covariance matrix, but also all the refinement

features, such as restrictions due to special positions or additional equations (site occupancies *etc.*). This method has been implemented into the *JANA*96 program package (Petricek, 1996). In Fig. 6 a p.d.f. map for Cu(2), the corresponding $p.d.f._{def}$ map and the error map for the p.d.f. are shown. The low level of the e.s.d.'s validates the deformation and therefore the model (notice that the $p.d.f._{def}$ map and the error map are plotted with the same contour interval). From the e.s.d.'s of the p.d.f. maps, the calculation of the error curve for the corresponding effective one-particle potentials is straightforward. The significance of the small effects in the potential curves given in the text have been checked with this procedure.

References

Bachmann, R. & Schulz, H. (1984). *Acta Cryst.* A**40**, 668–675.

Becker, P. J. & Coppens, P. (1974). *Acta Cryst.* A**30**, 129–147.

Bernardinelli, G. & Flack, H. D. (1985). *Acta Cryst.* A**41**, 500–511.

Boucher, F., Evain, M., Deniard, P. & Pfitzner, A. (1996). Unpublished results.

Bryndzia, L. T. & Davis, A. M. (1989). *Am. Mineral.* **74**, 236–242.

Burdett, J. K. & Eisenstein, O. (1992). *Inorg. Chem.* **31**, 1758–1762.

Charnock, J. M., Garner, C. D., Pattrick, R. A. D. & Vaughan, D. J. (1989). *J. Solid State Chem.* **82**, 279–289.

Cromer, D. T. (1974). *International Tables for X-ray Crystallography*, edited by J. A. Ibers & W. C. Hamilton, Vol. IV, pp. 149–150. Birmingham: Kynoch Press.

Cromer, D. T & Waber, J. T. (1974). *International Tables for X-ray Crystallography*, edited by J. A. Ibers & W. C. Hamilton, Vol. IV, pp. 72–98. Birmingham: Kynoch Press.

Daoudi, A., Lamire, M., Levet, J. C. & Noël, H. (1996). *J. Solid State Chem.* **123**, 331–336.

Flack, H. D. (1983). *Acta Cryst.* A**39**, 876–881.

Gotsis, H. J., Barnes, A. C. & Strange, P. (1992). *J. Phys. Condens. Matter*, **4**, 10461–10468.

Johnson, C. K. & Levy, H. A. (1974). *International Tables for X-ray Crystallography*, edited by J. A. Ibers & W. C. Hamilton, Vol. IV, pp. 311–336. Birmingham: Kynoch Press. (Present distributor Kluwer Academic Publishers, Dordrecht.)

Kanatzidis, M. G. & Sutorik, A. C. (1995). In *Progress in Inorganic Chemistry*, edited by K. D. Karlin, Vol. 43, pp. 151–265. New York: Wiley & Sons, Inc.

Karup-Møller, S. & Makovicky, E. (1974). *Am. Mineral.* **59**, 889–895.

Kuhs, W. F. (1984). *Acta Cryst.* A**40**, 133–137.

Kuhs, W. F. (1992). *Acta Cryst.* A**48**, 80–98.

Makovicky, E. & Balic-Zunic, T. (1995). *Can. Mineral.* **33**, 655–663.

Makovicky, E. & Skinner, B. J. (1979). *Can. Mineral.* **17**, 619–634.

Oliveria, M., McMullan, R. K. & Wuensch, B. J. (1988). *Solid State Ion.* **28**, 1332–1337.

Pauling, L. & Neuman, E. W. (1934). *Z. Kristallogr.* **88**, 54–62.

Petricek, V. (1996). *JANA*96. Institute of Physics, Academy of Sciences of the Czech Republic, Prague, Czech Republic.

Pfitzner, A. (1994). *Z. Anorg. Allg. Chem.* **620**, 1992–1997.

Pfitzner, A. (1996). Unpublished results.

Pfitzner, A. & Lutz, H. D. (1993). *Z. Kristallogr.* **205**, 165–175.

Sheldrick, G. M. (1993). *SHELXL*93. *Program for the Refinement of Crystal Structures*. University of Göttingen, Germany.

Sheldrick, G. M. (1996). *SHELXTLV*5. Siemens Analytical X-ray Instruments Inc., Madison, Wisconsin, USA.

Skinner, B. J., Luce, F. D. & Makovicky, E. (1972). *Econ. Geol.* **67**, 924–938.

Springer, G. (1969). *Neues Jahrb. Mineral. Monatsh.* pp. 24–32.

Tatsuka, K. & Morimoto, N. (1973). *Am. Mineral.* **58**, 425–434.

Van der Lee, A., Boucher, F., Evain, M. & Brec, R. (1993). *Z. Kristallogr.* **203**, 247–264.

Wuensch, B. J. (1964). *Z. Kristallogr.* **119**, 437–453.

Yude, Y., Boysen, H. & Schulz, H. (1990). *Z. Kristallogr.* **191**, 79–91.